ISSN 1061-8309, Russian Journal of Nondestructive Testing, 2022, Vol. 58, No. 8, pp. 679–688. © Pleiades Publishing, Ltd., 2022.
Russian Text © The Author(s), 2022, published in Defektoskopiya, 2022, No. 8, pp. 25–35.

ACOUSTIC METHODS

Immersion Testing of Curved Profile Objects by Surface Ultrasonic Waves

G. Ya. Dimkin[a,b,*], A. V. Kirikov[c,], and K. A. Bondarchuk[b,***]**

[a] *Research Institute of Bridges and Nondestructive Testing (AO NII Mostov), St. Petersburg, 190013 Russia*

[b] *Emperor Alexander I St. Petersburg State Transport University, St. Petersburg, 190031 Russia*

[c] *Nordinkraft AG, Remchingen, 75196 Germany*

**E-mail: gdymkin@gmail.com*

***E-mail: andrej.kirikov@nordinkraft.de*

****E-mail: bondarchukksenya1801@gmail.com*

Received June 7, 2022; revised July 2, 2022; accepted July 8, 2022

Abstract—A method for testing the products with a flat and curved surface using surface ultrasonic waves in the immersion version is proposed. Theoretical and experimental studies have shown that with the length of the testing zone from 20λ to 50λ, the combined application of the echo pulse method together with the amplitude and time variants of the shadow method makes it possible to detect both cracks and defects with a smooth profile with a depth of fractions of a wavelength on flat and curved surfaces. The research results were used in the development of an automatic rail monitoring system in the production flow; its tests confirmed high sensitivity and noise immunity of the immersion testing with surface waves.

Keywords: ultrasonic testing, surface wave, curved profile, immersion version, smooth profile defect, crack

DOI: 10.1134/S1061830922080034

INTRODUCTION

The eddy current method and nondestructive testing means implementing it are used to solve problems related to high-performance testing of the surface of long products, such as rails, under conditions of their industrial production. Their inherent disadvantages and limitations are low sensitivity in relation to certain types of defects, relatively low noise immunity in relation to the electromagnetic background of a metallurgical enterprise and residual magnetization of a test object, difficulties in using curved sections of the profile, the need to place eddy current sensors almost right up to the moving test object, as well as the small depth of penetration of eddy currents into ferromagnetic metals and alloys initiate intensive search for alternative methods and means of detecting surface and subsurface defects in long products.

One of such alternatives, potentially removing most of the limitations inherent to eddy current testing, is the use of surface ultrasonic waves.

Rayleigh-type surface ultrasonic waves are widely used in solving flaw detection problems [1]. From a practical point of view, the advantages of Rayleigh waves propagating along the free surface of a solid are primarily related to their localization in the surface layer and, consequently, high sensitivity to surface defects and an amplitude decay with distance slower than for bulk waves. Surface imperfections that occur both in the manufacture and operation of metal products (cracks, hairlines, slivers, prints, etc.) have diverse shape and not only lead to a change in the amplitude and time parameters of the transmitted signal, but also create scattered Rayleigh and bulk longitudinal and transverse waves, making it possible to use both echo-pulse and shadow methods of ultrasonic testing. It is also important that Rayleigh-type waves can propagate along curved (convex and concave) surfaces; this makes it possible to detect inhomogeneities on complex shaped surfaces [2].

At the same time, Rayleigh waves are characterized by high sensitivity to the contact of the surface with another medium [3], in particular to the presence of a liquid layer or local droplets and contaminants on the surface, resulting in scattering in the contact zone (which causes interference), as well as the transformation of a Rayleigh wave in the contact zone into an inhomogeneous wave carrying away energy into the medium in contact with the surface leading to a decrease in the length of the sounding surface area.

This disadvantage causes interest in the possibility of performing testing in the immersion version, i.e., when the test object is immersed in a liquid medium, which, of course, will reduce the length of the tested area, but at the same time exclude conditions for scattering of surface waves on local surface contamination.

Surface waves on the flat interface between a solid half-space and a liquid layer of finite and infinite thickness are theoretically and experimentally investigated in the works by I.A. Viktorov [5, 6], where analytical expressions are obtained and estimates of the dispersion of the phase velocity of waves and attenuation are given. The regularities and efficiency of the transformation of surface waves into bulk longitudinal waves emitted into a liquid in contact with a solid were studied in [7], where the authors limited themselves to solving a two-dimensional problem. The finiteness of the emitter size in the plane perpendicular to the plane of incidence determines the direction of the field of the excited Rayleigh wave, studied by I.A. Viktorov [8] in relation to the pulse mode.

Studies of the interaction patterns of Rayleigh waves with rectangular slits and semicylindrical grooves, as well as their propagation over a surface of complex geometry (for example, sawtooth or rough) are presented, in particular, in the experimental works [9, 10]. It was shown in [11] that for a rectangular groove of shallow depth, the reflection coefficients (R_d) and transmission coefficients (D_d) in steel and duralumin differ only slightly; this allows one to compare experimental data obtained for the air-steel interface under laboratory conditions and the data obtained in [9] for the air-duralumin boundary.

The presence of these fundamental theoretical and experimental results creates the necessary basis for studying echo-pulse and shadow methods of the immersion testing of products with a nonplanar surface with surface quasi-Rayleigh waves.

In order to study the patterns of propagation, reflection, and passage of surface waves when the product is located in an immersion medium, consider a solid body located in a liquid, with the body surface having flat and cylindrical (convex or concave) sections. A surface wave excited on a flat section of the solid by the wedge method using a straight piezoelectric transducer located in the immersion liquid at the Rayleigh angle propagates in a direction perpendicular to the cylinder generatrix, encountering a surface defect in the form of a narrow rectangular (crack model) or semicylindrical (roughness model) groove located on a curved or flat surface area oriented perpendicular to the wave propagation direction and covering the entire width of the surface wave beam.

Further, let us consider acoustic paths for this problem. When deriving analytical expressions for the amplitudes of the shadow and echo signal, we assume that: a homogeneous, isotropic and ideally elastic solid is located in an ideal liquid; the curvature radius of the solid surface is much larger than the wavelength; the path from the emitting and receiving transducers to the surface of the solid traversed by a wave in the liquid does not exceed the value of the near zone of the transducer; and defect models are located in the localization layer of surface waves (approximately one and a half wavelengths) and are removed from the points of excitation and reception of surface waves at a distance considerably exceeding the wavelength. The possible length of the acoustic path during immersion testing by surface waves (the test zone size) is determined by the attenuation of surface waves due to emission into the liquid [5]. The theoretical and experimental evaluation of a drop in the amplitude of a surface wave with distance (Fig. 1) shows that in the immersion version of testing, the presence of a thick layer of liquid on the surface of the product dramatically (from 0.01 to 0.5–0.6 dB per wavelength) increases the attenuation of the amplitude of the propagating surface wave. At the same time, the physical properties of the immersion liquid have a negligible effect on the attenuation of a surface wave and, accordingly, on the possibilities of ultrasonic testing.

Thus, the length of the effective zone of immersion testing by surface waves for the applied testing methods ranges from 20λ to 50λ and, with practically realizable parameters (active zone size, frequency, distance to the test object in the immersion liquid) of the ultrasonic transducer, is mainly in the near field zone. In order to solve the engineering problems set out in this paper, we will limit the analysis of the acoustic path to the energy approximation, which gives sufficient accuracy.

Experimental studies of methods of immersion testing by surface waves carried out in this paper to verify and supplement theoretical estimates were performed using dedicated flaw detection equipment and serial devices, piezoelectric transducers for contact and immersion testing with operating frequencies of 1–3 MHz, and an immersion bath with positioning mechanisms. Grooves of rectangular and cylindrical shape were made in steel research samples at various depths by milling. All measurements were performed repeatedly while excluding sharply deviating values. The average values and 95% confidence intervals shown in the figures with experimental data were calculated according to the measurement data.

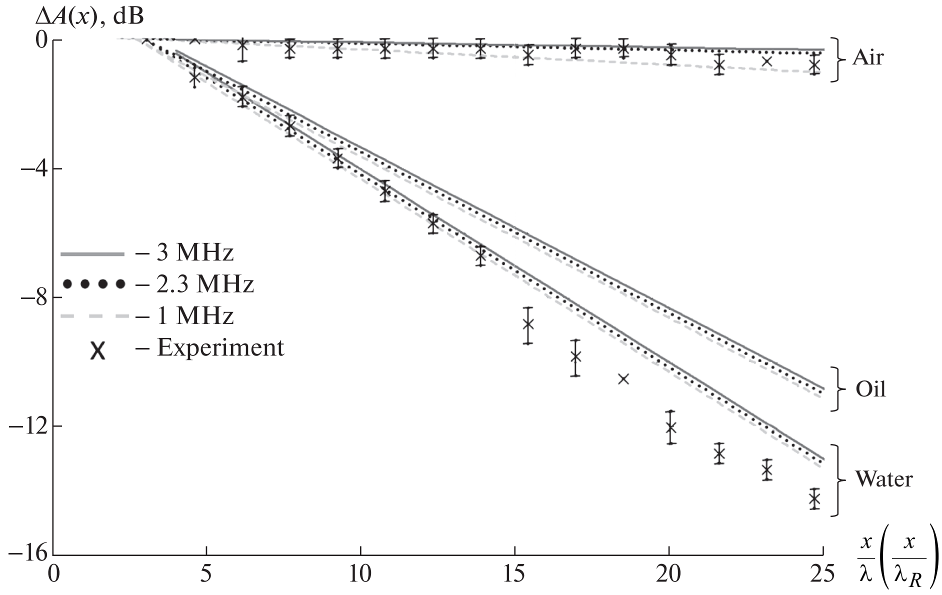

Fig. 1. Attenuation of surface wave amplitude with distance.

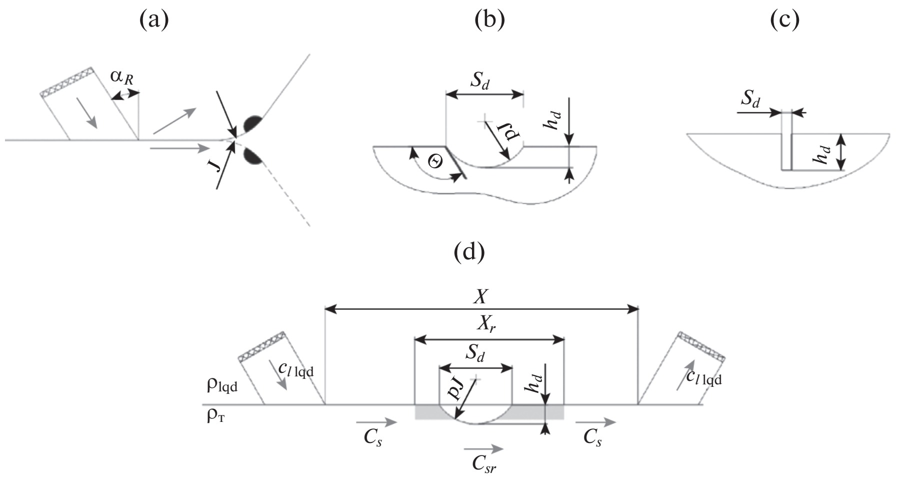

Fig. 2. General scheme of the acoustic path of the shadow method of surface wave testing (a); defect models: semicylindrical groove (b), rectangular groove (c); acoustic path model (d).

SHADOW METHOD

The presence of surface damage causes a change in both the amplitude and time parameters of the pulses of surface ultrasonic waves propagating through a product section. Recording these changes, which are a sign of the presence of a defect, is the basis of the amplitude and time shadow methods.

Figure 2 shows a general scheme, defect models, and a model of the acoustic path in the shadow method on which a curved section of the solid is marked.

The following designations are used in the figure: ρ_{lqd} and ρ_{sld} are the densities of the liquid and the solid, respectively; $s_{l\,\text{lqd}}$ is the velocity of a longitudinal wave in the liquid; c_S and c_{Sr} are the velocities of surface waves in the solid bordering the liquid on its flat and curved surfaces, respectively; x is the length of the acoustic path (from the emitter to the receiver) covered by a surface wave; and x_r is the length of a curved (convex or concaved) cylindrical section of the surface with radius r.

The acoustic path in the amplitude shadow method is characterized by the ratio of the amplitude of the signal that has passed a path with a defect (A_d^{Sh}) to the amplitude of the signal in the defect-free section (A_0^{Sh}), that is, by the defect detection coefficient:

$$K^{\mathrm{Sh}} = A_d^{\mathrm{Sh}}/A_0^{\mathrm{Sh}}. \tag{1}$$

In the energy approximation, we write the intensity I_d^{Sh} of the surface wave signal that has passed through the acoustic path shown in Fig. 2d in the form of:

$$I_d^{\mathrm{Sh}} = I_{\mathrm{e}}\tilde{Q}(b,x)\tilde{D}_d(h_d,s_d)\tilde{K}_a(b)\tilde{\Psi}(x,r,x_r), \tag{2}$$

where I_{e} is the intensity of the wave emitted into the solid and $\tilde{Q}(b,x)$ is the coefficient characterizing the decrease in intensity due to the divergence of the surface wave beam during propagation. For the near zone, where the wave front can be considered flat, $\tilde{Q}(b,x)=1$ and for the far zone (cylindrical front), $\tilde{Q}(b,x)=\frac{b^2}{\lambda x}$; $\tilde{D}_d(h_d,s_d)$ is the coefficient of transmission through the defect in terms of intensity; $\tilde{K}_a(b)$ is the coefficient of the axial concentration of the field of surface waves emitted by the transducer of width b, which takes the value $\tilde{K}_a=1$ for the near zone and $\tilde{K}_a=\frac{0.5\left(\frac{2\pi}{\lambda}\right)^2 b}{\cos\left(\frac{2\pi}{\lambda}b\right)+\frac{2\pi}{\lambda}b\cdot Si\left(\frac{2\pi}{\lambda}b\right)-1}$ for the far zone; $\tilde{\Psi}(x,r,x_r)$ is the coefficient characterizing the decrease in intensity due to the attenuation of the surface wave as it propagates along the boundary with the liquid (see Fig. 1) and the re-emission of bulk waves on a section of the concave curved surface [4].

The energy losses and, accordingly, the values of the transmission coefficients when a surface wave bends crack-like and shallow defects are caused by reflection of the surface wave from the bends (angles) of the surface encountered in its path, additional attenuation due to the emission of bulk waves when the wave propagates along a concave section of the surface, as well as scattering in the form of bulk waves resulting from diffraction by sharp angles and areas with a radius less than the wavelength [12].

Taking into account the adopted assumptions and the expressions for losses at the liquid boundary and on the concave curved surface in [4, 7], the formulas for the shadow signal amplitudes and detection coefficients of extended rectangular $\left(K_{d\,\mathrm{rct}}^{\mathrm{Sh}}\right)$ and semicylindrical $\left(K_{d\,\mathrm{cld}}^{\mathrm{Sh}}\right)$ grooves oriented perpendicular to the beam can be written as

$$K_{d\mathrm{rct}}^{\mathrm{Sh}} = D_{d\mathrm{rct}}, \tag{3}$$

where $D_{d\,\mathrm{rct}}$ is the amplitude transmission coefficient for the narrow rectangular groove of shallow depth, the expression for which is obtained in [10];

$$K_{d\mathrm{cld}}^{\mathrm{Sh}} = \exp[-(\alpha_R+\alpha_S)(s_{dr_d}-s_d)+\alpha_{Sr}s_d-\alpha_{Sr_d}s_{dr_d}], \tag{4}$$

where α_R and α_S are the attenuation coefficients of the surface wave when propagating along the solid-air and solid-liquid interface, respectively; α_{Sr} and α_{Srd} are the coefficients of additional attenuation of the surface wave on concave cylindrical sections of the surface with radii r and r_d, respectively, providing, as follows from [4, 9], acceptable accuracy for both large and small wave radii of curvature; and s_{dr_d} is the path length along the surface of the groove.

It should be noted that the above formulas do not take into account the diffraction effects leading to the transformation of surface waves into bulk ones scattered by a defect.

The results of experimental studies on the dependence of the amplitude attenuation of the shadow signal on the depth of rectangular and semicylindrical grooves performed in this work, as well as the data calculated according to (3) and (4) presented in [9], are shown in Fig. 3.

It can be seen that the experimental data for the detection coefficients of a rectangular groove on the free surface of the steel sample and during immersion testing (see Fig. 3) are in satisfactory agreement with the calculations by formula (3) for small defect depths and with the results obtained in [9] for aluminum samples. The difference between the theoretical results and the experimental data for groove depths

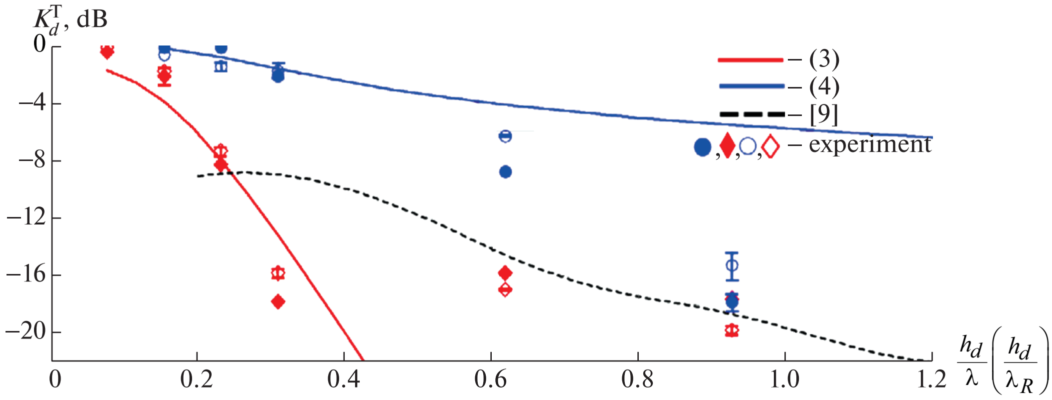

Fig. 3. Detection coefficients of narrow ($s_d/\lambda \to 0$) rectangular (♦, ◇) and semi-cylindrical ($s_d/\lambda \approx 5$) (●, ○) grooves of depth h_d with the shadow method of surface wave testing: ◇, ○ steel–air; ♦, ● steel–water.

greater than half the wavelength is, apparently, due to the use of an approximation that does not take into account the influence of waves that bypass the crack (rectangular groove) propagating along its edges. With an increase in the ratio h_d/s_d, the detection coefficients for a rectangular (crack-like) and smooth groove with a semi-cylindrical bottom become close.

In the course of experimental studies of the shadow method, it was also found that a decrease in the efficiency of excitation of a surface wave in the case where the defect is in the zone of the incident beam has a more significant effect on the amplitude of the shadow signal than scattering of the propagating surface wave by the defect. This effect, which manifests itself in a decrease in the coefficient of conversion of a longitudinal wave in the liquid into a surface wave, is a "parametric" effect that is predetermined by the shape of the surface defect and the ratio of the defect size to the excitation zone and is not amenable to analytical evaluation, but can be effectively used in practical testing.

The results of the conducted studies of the acoustic path of the amplitude shadow method of immersion testing by surface waves show that:

1. The detection coefficients of crack-like (rectangular groove) and smooth (semicylindrical groove) surface defects depend weakly on the acoustic characteristics of the metal and the medium the tested surface is in contact with.

2. When the metal product is located both in air and in water, the detectability coefficient acceptable for practical problems of flaw detection is provided for defects perpendicular to the wave propagation direction with a depth of more than (0.3–0.5)λ.

To assess the influence of the groove geometry and size on the time shift Δt of the transmitted surface wave pulse, which is a sign of a defect in the time-domain shadow method, we calculate the propagation time assuming [4] that the trajectory of the pulse propagation repeats the defect shape.

In this case, assuming that the surface wave propagates successively along the front and back faces of the rectangular groove with a negligible opening ($s_d \to 0$), the difference between the propagation times of the signal in the defective and defect-free sections can be determined using the simple formula

$$\Delta t_{\text{rct}} = \frac{2h_d}{c_S} - \frac{s_d}{c_S} \approx \frac{2h_d}{c_S}. \tag{5}$$

For a semicylindrical groove, it is also necessary to take into account the fact that the velocity of a surface wave on the curved groove surface depends on the curavture radius, while the velocity correction, according to [4, 9], is valid for both small and large radii. At the same time, in the range of the practically important groove radii, the change in the velocity of the surface wave is negligible (less than 0.04).

Calculating the length s_{dr_d} of the pulse path along the surface of the semicylindrical groove with width s_d and depth h_d and using the results in [4], we obtain analytical expressions for the propagation time of surface waves along the section containing the groove that allow one to analyze the pat-

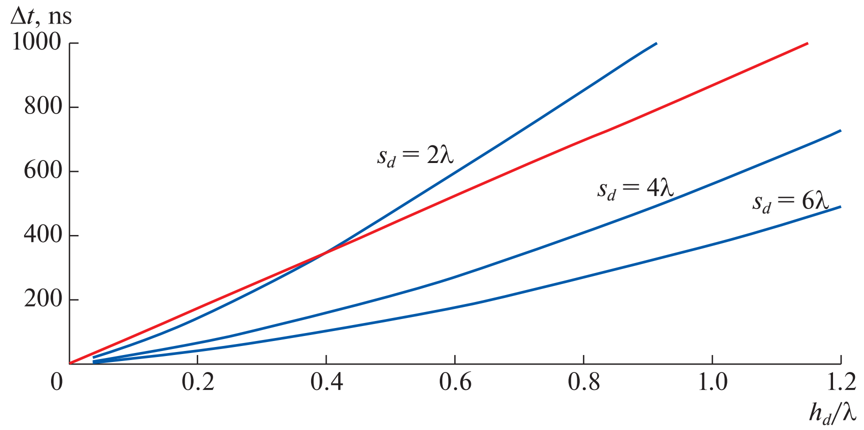

Fig. 4. Dependence of the time shift of a transmitted surface wave signal on the wave depth h_d/λ of rectangular (——) and semicylindrical (——) grooves.

terns of the influence of the groove size on the time shift (Δt_{r_d}) of the transmitted signal recorded by the shadow method,

$$\Delta t_{r_d} = \frac{\pi\left(\frac{s_d^2 + 4h_d^2}{8h_d}\right)\arcsin\left(\frac{4h_d s_d}{s_d^2 + 4h_d^2}\right)}{90}\frac{1}{c_R} \times \left[1 - \frac{\left[1 + \frac{s}{q} + \frac{k_S e_q}{2se_S}\left(1 - \frac{s^2}{q^2}\right)\right] + \left[1 + \frac{s}{q} - \frac{k_R e_S}{2se_q}\left(1 - \frac{s^2}{q^2}\right)\right] - \frac{2s^2}{k_t^2}\left(\frac{k_t^2}{k_l^2} - 1\right)}{k_R r_d\left[\left(1 - \frac{s}{q}\right)\left(\frac{e_q}{e_S} - \frac{e_S}{e_q}\right) + \frac{4k_R s}{k_t^2}\left(\frac{k_t^2}{k_l^2} - 1\right)\right]}\right]^{-1} - \frac{s_d}{c_R}, \quad (6)$$

where $s = \sqrt{k_R^2 - k_t^2}$; $q = \sqrt{k_R^2 - k_t^2}$; $e_q = \exp[2\,\text{arccoth}(q/k_R)]$; $e_s = \exp[2\,\text{arccoth}(q/k_R)]$; and k_t, k_l and k_S are the wave numbers of transverse, longitudinal, and surface waves, respectively.

The result of calculation using expression (6) is shown in Fig. 4.

The analysis of the time version of the shadow method allows one to conclude that the dependence of the time shift (delay) of a surface wave pulse during its passage through both rectangular and semicylindrical grooves depends almost linearly on the wave groove depth h_d/λ and that the time shift decreases considerably with an increase in the semicylindrical groove width.

Figure 5 shows the dynamic envelopes of the amplitude and time shift of a signal received during testing that has passed over the surface of the product containing two defects.

It can be seen that the decrease in the amplitude of the past (shadow) signal is accompanied by an increase in its propagation time; this confirms the effectiveness of the joint use of amplitude- and time-domain versions of the shadow method of surface wave testing. Recording two parameters helps improving the noise immunity of testing and provides potential opportunities for assessing the depth (size) of the detected defect.

ECHO PULSE METHOD

For an echo method of testing by a single crystal probe for an infinitely extended groove, we can adopt an acoustic path model that differs from the above model for the shadow method in that there is a need to take into account not the coefficient of transmission but the coefficient of reflection from the defect, and the geometric difference is that for the echo method, the distances traveled by the wave on all sections of the path from the emitter to the defects and back are equal (Fig. 6).

(a)

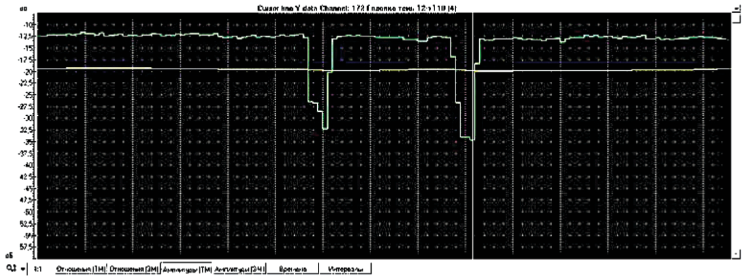

(b)

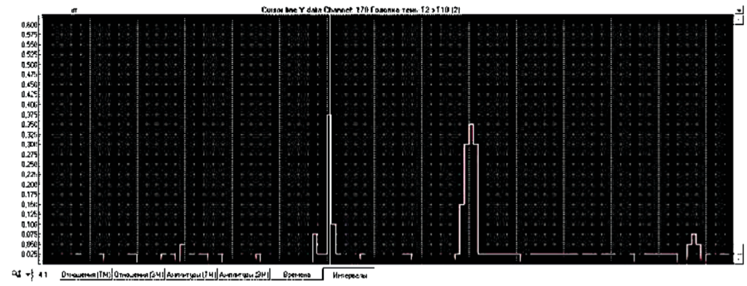

Fig. 5. Dynamic envelopes of the amplitude (a) and time shift (b) of the shadow signal when moving along the product surface containing two defects.

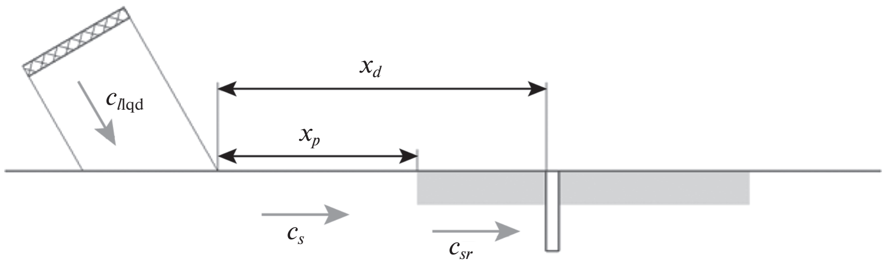

Fig. 6. Model of the acoustic path of the echo method of ultrasonic testing by surface waves.

By analogy with the expression given earlier for the shadow method (2), we write the intensity of the echo signal due to defect in the form

$$I_d^{\text{echo}} = I_{\text{e}}\tilde{Q}(b, x_d)\tilde{R}_d(h_d, s_d)\tilde{K}_a(b)\tilde{\Psi}(x_d, x_p, r). \tag{7}$$

When the defect is located on the transducer's acoustic axis, $\tilde{K}_a = 1$. In this case, for the far zone, the amplitude of the echo signal can be written as

$$A_d^{\text{echo}} = A_{\text{e}}(1/x_d)R_d \exp[-2(\alpha_R + \alpha_S)x_d - 2\alpha_{Sr}(x_d - x_p)]. \tag{8}$$

At distances not exceeding the value of the near zone of the transducer, for which $\tilde{Q}(b, x_d) = 1$, the amplitude of the echo signal takes the form:

$$A_d^{\text{echo}} = A_{\text{e}}R_d \exp[-2(\alpha_R + \alpha_S)x_d - 2\alpha_{Sr}(x_d - x_p)]. \tag{9}$$

In actual testing, sensitivity adjustment is performed based on the echo signal from a reference reflector. It is customary to use a right dihedral angle in a sample of the tested material as a reference reflector for surface waves [13]. Let us assume that the distance from the excitation–reception point of surface waves to the reference reflector is chosen to be minimally sufficient for separate observation and measurement of the probing and reflected pulses. In this case, the effect of attenuation of surface waves is practically absent even in the case of contact of the surface with the liquid, $\Psi = 1$. To assess the possible influ-

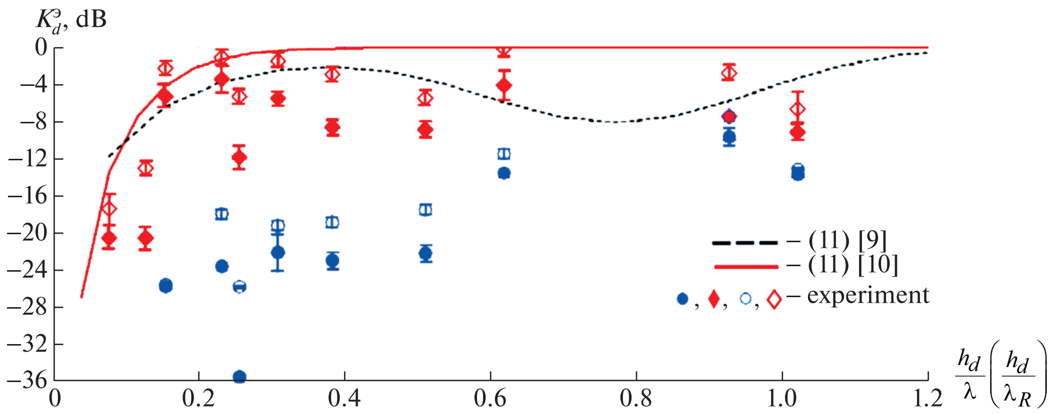

Fig. 7. Coefficients of detection of narrow ($s_d/\lambda \to 0$) rectangular (◆, ◇) and semicylindrical ($s_d/\lambda \approx 5$) (●, ○) grooves of depth h_d with the echo method of surface wave testing: ◇, ○ steel–air; ◆, ● steel–water.

ence of contact with the liquid on the reflection coefficient of a surface wave from the right dihedral angle (R_{inf}), an experiment was conducted that did not show any considerable change in the amplitude of the echo signal from the right dihedral angle when the sample was immersed in water. In this regard, (R_{inf}) is assumed to be equal to the value obtained for a Rayleigh wave [11] and the amplitude A_0 of the reference echo signal from the reference reflector equal to

$$A_0 = 0.67A_{\mathrm{e}}. \tag{10}$$

As a result, taking into account [7], for the coefficient of detection of a defect located in the transducer near field zone we obtain

$$K_d^{\mathrm{echo}} = 3/2R_d \exp[-2(\alpha_R + \alpha_S)x_d - 2\alpha_{Sr}(x_d - x_p)]. \tag{11}$$

The resulting general expression can be used for a detailed analysis of the acoustic path of the echo-pulse immersion testing by surface waves.

For a defect model in the form of a rectangular groove, it should be supplemented with the formulas for R_d in [11].

The calculation results and the experimental values for the coefficient of detection of rectangular and semicylindrical grooves on a flat surface in air and in water are shown in Fig. 7.

There is a satisfactory qualitative and quantitative agreement between the results of experiments performed in this paper with the theoretical and experimental data by other authors [9, 11]. At the same time, the absence of oscillations on the calculated curve for a rectangular groove is explained, just as for the shadow method, by the energy approximation used in [11].

It can be seen from Fig. 7 that the detection coefficients for the options of testing in air and in an immersion medium differ only slightly; the detectability of a semicylindrical groove by the echo method is close to the detectability of a rectangular groove at depths of a wavelength or more; the values of detection coefficients acceptable for practical purposes are provided for crack-like defects deeper than 0.2λ and defects with a smooth profile deeper than 0.6λ.

The effect of the width of a smooth defect on its detectability is illustrated by the data presented in Fig. 8. As can be seen, both the echo-pulse and amplitude shadow methods critically reduce the detectability of semicylindrical grooves the width of which exceeds the depth by an order of magnitude or more.

Based on the performed studies of immersion ultrasonic testing by surface waves,

– The possibility of using the echo-pulse method, as well as the amplitude- and time-domain variants of the shadow method for immersion surface-wave testing of flat and curved (convex and concave) surfaces of products of complex cross-sectional shape has been substantiated.

– A technique for combined application of the methods is developed and the requirements for the equipment of immersion ultrasonic testing by surface waves for detecting defects with a smooth profile and crack-like surface defects with a depth of fractions of wavelength are substantiated.

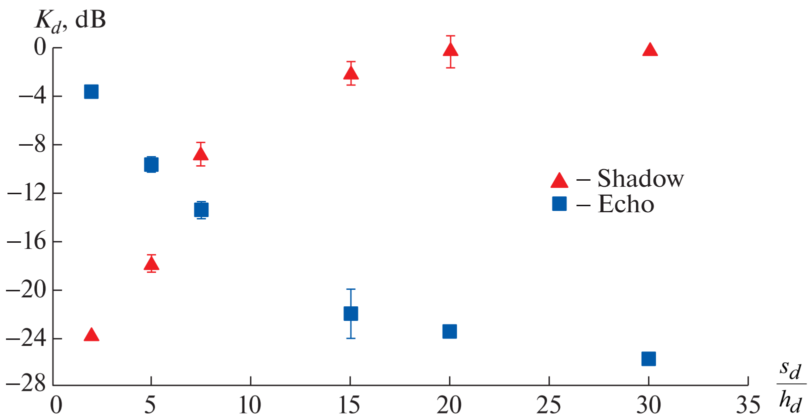

Fig. 8. Dependence of detection coefficients for the echo and shadow methods on the relative width of semicylindrical groove.

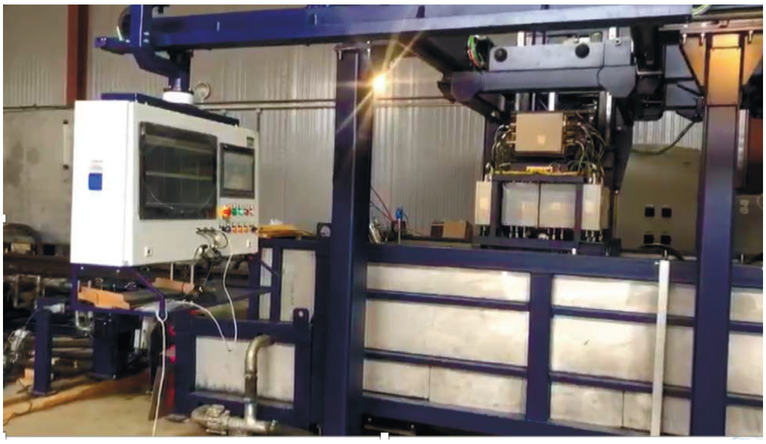

Fig. 9. General appearance of the NORDINSCAN-RAIL-S (Nordinkraft) installation of ultrasonic quality control of rail surface in the line of acceptance testing of rails at a metallurgical enterprise.

– The NORDINSCAN-RAIL-S installation was created (Fig. 9) (Nordinkraft) for automatic immersion ultrasonic quality control of the rail surface, including a multichannel flaw detection hardware and software complex with piezoelectric phased antenna array blocks [14] that allows one to perform acceptance testing of railway rails and rail rolling of all types in the production flow in order to detect defects along the entire perimeter of the surface (including in areas inaccessible to eddy current testing).

Figure 10 shows examples of real defects (cracks, prints, slivers, shells, and grooves) identified using the techniques and equipment described in the article.

CONCLUSIONS

The results of the research presented in the article and its implementation in the creation of equipment and technology for ultrasonic monitoring of rails in order to identify surface defects

– Have formed a methodological basis for the combined application of the echo-pulse method together with amplitude- and time-domain variants of the shadow method of immersion testing by surface waves.

– Have shown a high sensitivity, an increased noise immunity, and additional capabilities for testing curved surfaces of complex shaped products using immersion technology of surface ultrasonic waves.

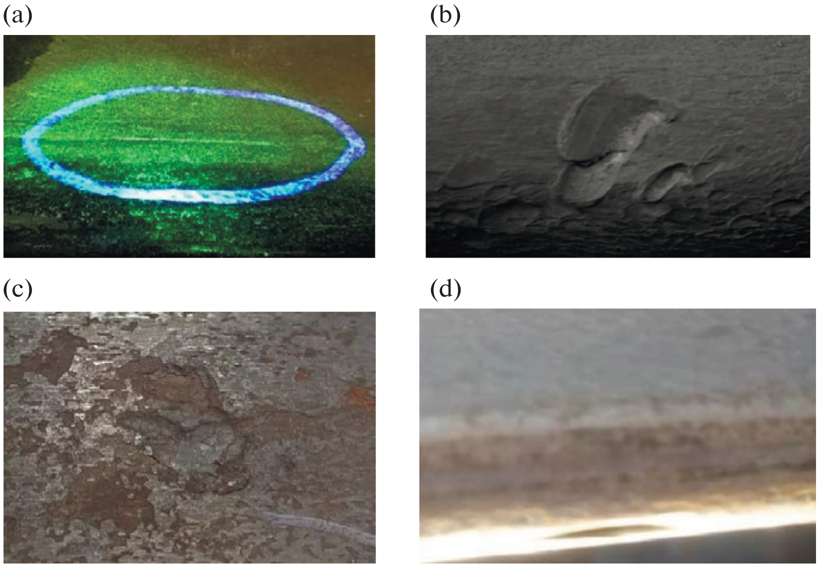

Fig. 10. Examples of unacceptable surface metallurgical defects of rails detected during immersion testing by surface waves: (a) 30-mm–long mark on the rolling surface in the rolling direction (a); (b) ~12 × 10 mm imprint at depth 1.0 mm on the head rolling surface; (c) ~12 × 17 mm sliver at depth 0.8 mm on the foot; (d) crack on the edge of the rail foot blade.

– Have expanded the possibilities of using ultrasonic surface waves for problems of flaw detection with the underwater position of a test object and in immersion techniques.

REFERENCES

1. Polupan, A.V., *Ul'trazvukovoi kontrol' poverkhnostnymi volnami* (Ultrasonic Testing by Surface Waves), Moscow: Spektr, 2014.
2. Zhostkov, R.A., Reconstruction of inhomogeneities of a medium during microseismic sounding along a curvilinear surface, *Acoust. Phys.,* 2019, vol. 65, no. 5, pp. 611–622.
3. Baev, A.R., Panteleenko, F.I., Zakharenko, V.V., Razmyslovich, G.I., Zhavoronkov, K.G., and Gil', N.N., Transformation and scattering of surface waves on acoustic load for ultrasonic monitoring and measurements. Part 1. Sliding boundary of acoustic contact, *Prib. Metod. Izmer.,* 2018, vol. 9, no. 1, pp. 18–39.
4. Viktorov, I.A., Rayleigh-type waves on cylindrical surfaces, *Akoust. Zh.,* 1958, no. 2, pp. 131–136.
5. Viktorov, I.A., Grishchenko, E.K., and Kaekina, T.M., Investigation of the propagation of ultrasonic surface waves at the boundary of a solid body with a liquid, *Akoust. Zh.,* 1963, no. 2, pp. 162–170.
6. Viktorov, I.A., On the calculation of the phase velocities of surface waves at the boundary of a solid half-space with a liquid layer, *Akoust. Zh.,* 1977, no. 6, pp. 947–948.
7. Nikiforov, L.A. and Kharitonov, A.V., Excitation of a surface wave by an ultrasonic beam at the liquid–solid interface, *Defektoskopiya,* 1973, no. 3, pp. 45–53.
8. Viktorov, I.A. and Zubova, O.M., On the radiation patterns of Lamb and Rayleigh wave emitters, *Akoust. Zh.,* 1963, no. 2, pp. 171–175.
9. Viktorov, I.A., On the influence of surface imperfections on the propagation of Rayleigh waves, *Dokl. Akad. Nauk USSR,* 1958, vol. 119, no. 3, pp. 463–465.
10. Zharilkapov, S.Zh. and Krilov, V.V., Rayleigh wave scattering on a recess of arbitrary depth, *Akoust. Zh.,* 1987, no. 5, pp. 878–883.
11. Danilov, V.N. and Yamshchikov, V.S., On the scattering of Rayleigh surface waves by boundary defects, *Akoust. Zh.,* 1985, no. 3, pp. 323–327.
12. Akhromeeva, I.D. and Krylov, V.V., Transformation of Rayleigh waves into volumetric waves on local surface defects, *Akoust. Zh.,* 1977, no. 4, pp. 510–516.
13. Damaskin, A.L., Dymkin, G.Ya., and Kostyuk, O.M., Investigation of the acoustic tract in echo-pulse testing by surface waves, *Defektoskopiya,* 1991, no. 2, pp. 26–30.
14. Kirikov, A.V. and Dymkin, G.Ya., RF Patent no. 2723913, 2020.

SPELL: OK